

On local analysis of instability by magnetic buoyancy

By M. P. GIBBONS†

Department of Mechanical Engineering, The City University, London, U.K.

(Received 4 March 1981 and in revised form 17 August 1981)

Moffatt's (1978) model for instability, by magnetic buoyancy, of a rotating layer of compressible fluid is extended to demonstrate that local stability analysis, theoretically valid for only a shallow layer, can still be useful for predicting instability when the layer is deep.

1. Introduction

Certain stability problems in magnetohydrodynamics (see Acheson 1978 and references therein) reduce to finding the complex eigenvalues \bar{c} of the differential equation

$$\frac{d^2 f}{d\bar{z}^2} + [\lambda^2 q_0(\bar{z}, \bar{c}) + q_2(\bar{z}, \bar{c})] f = 0, \quad (1.1)$$

subject to the boundary conditions

$$f(\bar{z}_1) = f(\bar{z}_2) = 0. \quad (1.2)$$

Here λ is a parameter, and \bar{z} has been made dimensionless with respect to a scale height.

The complexity of the coefficients q precludes a general analytic solution of (1.1), but in the limit $\lambda \rightarrow \infty$ the solution can be deduced (Nayfeh 1973) from the WKBJ approximation:

$$f = q_0^{-\frac{1}{2}} \{ \bar{a} \exp(\lambda i \theta) + \bar{b} \exp(-\lambda i \theta) \}, \quad (1.3)$$

where \bar{a} , \bar{b} are complex constants, and

$$\theta(\bar{z}) = \int_{\bar{z}_1}^{\bar{z}_2} (q_0(\tau))^{\frac{1}{2}} d\tau \quad (1.4)$$

(it is sufficient, for the purposes of this paper, to assume that there are no turning points). Then (1.2) is satisfied if N is an integer and

$$\int_{\bar{z}_1}^{\bar{z}_2} q_0^{\frac{1}{2}} d\bar{z} = N\pi/\lambda. \quad (1.5)$$

In general, (1.5) is a pair of nonlinear equations for the real and imaginary parts of \bar{c} and must be solved numerically, a process which is scarcely more efficient than numerical solution of (1.1). When $|\bar{z}_2 - \bar{z}_1| \ll 1$, (1.5) may be approximated by

$$q_0(\bar{z}_c) = \frac{N^2 \pi^2}{\lambda^2 (\bar{z}_2 - \bar{z}_1)^2}, \quad (1.6)$$

where $\bar{z}_c = \frac{1}{2}(\bar{z}_1 + \bar{z}_2)$; the question remains, however, of how well this local analysis approximates the eigenvalues of (1.1) when $|\bar{z}_2 - \bar{z}_1| \sim O(1)$. We address this matter here, by solving (1.1) numerically in a particular case and comparing the true eigenvalues (obtained in §4) with those predicted by local analysis (see §3);

† Present address: Marlborough College, Wiltshire, SN8 1PA, U.K.

attention is confined to a simple model for instability by magnetic buoyancy, which is now described.

2. Mathematical formulation

Consider, therefore, a layer of isothermal, inviscid, compressible fluid, of density $\rho_0(z)$, which is a perfect conductor of electricity and rotates with constant angular velocity $\mathbf{\Omega} = -\Omega \mathbf{e}_x$, where $\Omega > 0$ and $\mathbf{e}_x, \mathbf{e}_y$ and \mathbf{e}_z are unit vectors in the x -, y - and z -directions respectively of a rotating Cartesian frame of reference. The fluid is unbounded in directions x and y but bounded by plane walls at $z = z_1, z_2$. A magnetic field of flux density $\mathbf{B}_0 = B(z) \mathbf{e}_y$ permeates the fluid, which is therefore in equilibrium under gravity $\mathbf{g} = -g(z) \mathbf{e}_z$, provided

$$a^2 \frac{d\rho_0}{dz} + \frac{B}{\mu} \frac{dB}{dz} + \rho_0 g = 0. \tag{2.1}$$

Here μ and a are respectively the constant magnetic permeability and isothermal sound speed. We can rewrite (2.1) in the form

$$\frac{1}{\rho_0} \frac{d\rho_0}{dz} = -(a^2 + \frac{1}{2} V^2)^{-1} \left(g + V \frac{dV}{dz} \right), \tag{2.2}$$

where $V(z) \equiv B(z)[\mu\rho_0(z)]^{-\frac{1}{2}}$ is the Alfvén speed; (2.2) determines the stratification once the dependence of V on height has been prescribed. We shall assume that z_1 and z_2 are no more than a scale height apart, and take g to be constant. The system we have just described is potentially unstable by the mechanism of magnetic buoyancy, as described by Moffatt (1978, §10.7).

Perturbations to the equilibrium (2.1) are governed by the linearized forms of the momentum equation, of Gauss’s law and the continuity equation and of the magnetic induction equation. In nonlinear form these equations are

$$\left. \begin{aligned} \rho^* \left(\frac{d\mathbf{u}}{dt} + 2\mathbf{\Omega} \wedge \mathbf{u} \right) &= -a^2 \nabla \rho^* + \frac{1}{\mu} (\nabla \wedge \mathbf{B}^*) \wedge \mathbf{B}^* + \rho^* \mathbf{g}, \\ \frac{d\rho^*}{dt} + \rho^* \nabla \cdot \mathbf{u} &= 0, \quad \nabla \cdot \mathbf{B}^* = 0, \quad \frac{\partial B^*}{\partial t} = \nabla \wedge (\mathbf{u} \wedge \mathbf{B}^*), \end{aligned} \right\} \tag{2.3}$$

where $t, \mathbf{u} = (u, v, w), \rho^*$ and \mathbf{B}^* denote time, fluid velocity, fluid density and magnetic flux density respectively. We confine attention to the low-frequency perturbations by setting $d/dt = 0$ in the momentum equation (to filter out inertial and pure Alfvén waves) and $\partial/\partial t = 0$ in the continuity equation (to filter out acoustic and magneto-acoustic waves). We obtain in this manner the linearized equations

$$\left. \begin{aligned} 0 &= -\frac{\partial}{\partial x} \left(a^2 \rho + \frac{B b_y}{\mu} \right) + \frac{B}{\mu} \frac{\partial b_x}{\partial y}, \\ 2\rho_0 \Omega w &= -a^2 \frac{\partial \rho}{\partial y} + b_z B' / \mu, \\ -2\rho_0 \Omega v &= -\frac{\partial}{\partial z} \left(a^2 \rho + \frac{B b_y}{\mu} \right) + \frac{B}{\mu} \frac{\partial b_z}{\partial y} - \rho g, \\ \frac{\partial}{\partial t} \mathbf{b} &= B \frac{\partial \mathbf{u}}{\partial y} - \mathbf{B}_0 \nabla \cdot \mathbf{u} - w B' \mathbf{e}_y, \\ \rho_0 \nabla \cdot \mathbf{u} + \rho'_0 w &= 0, \end{aligned} \right\} \tag{2.4}$$

to which we seek solutions of the form

$$[\mathbf{u}, \mathbf{b}, \rho] = \mathcal{R}[\hat{\mathbf{u}}, \hat{\mathbf{b}}, \hat{\rho}] \exp i(kx + my - \omega t). \quad (2.5)$$

Here $\mathbf{b} = (b_x, b_y, b_z)$ and ρ are the perturbations in magnetic flux and fluid density, $\omega = \omega_{\mathbf{R}} + i\omega_{\mathbf{I}}$ is the (complex) angular frequency, k and m are wavenumbers in the directions of $\mathbf{\Omega}$ and \mathbf{B}_0 , and, throughout the paper, a prime denotes ordinary differentiation of a function with respect to its argument, in this case z . By eliminating all variables in favour of \hat{w} we obtain a second-order ordinary differential equation for $f \equiv B\hat{w}$:

$$f'' + [\omega^2 A_0 + \omega A_1 + A_2] f = 0, \quad (2.6)$$

where

$$A_0(z) \equiv 4\Omega^2 k^2 / m^4 V^4, \quad (2.7)$$

$$A_1(z) \equiv \frac{2\Omega}{m^3 V^2} \left(k^2 \frac{\rho'_0}{\rho_0} - g \frac{s^2}{a^2} \right), \quad (2.8)$$

$$A_2(z) \equiv -s^2 \left(1 + \frac{gB'}{m^2 a^2 B} \right) - \frac{B''}{B}, \quad (2.9)$$

$$s^2 \equiv k^2 + m^2. \quad (2.10)$$

To write (2.6) in the dimensionless form (1.1) we set

$$z = \frac{a^2 \bar{z}}{g}, \quad (k, m) = \frac{g}{a^2} (\bar{k}, \bar{m}), \quad \omega = \frac{V_0^2 g^2 \bar{\omega}}{2\Omega a^4}, \quad (2.11)$$

$$V = V_0 \bar{V}(\bar{z}), \quad \bar{D} = 1 + \frac{1}{2} \Gamma \bar{V}^2, \quad (2.12)$$

$$\Gamma = V_0^2 / a^2, \quad \lambda = \frac{k}{m} = \frac{\bar{k}}{\bar{m}}, \quad \bar{c} = \bar{\omega} / \bar{m}, \quad (2.13)$$

and define

$$\left. \begin{aligned} \bar{\phi}(\bar{z}) &\equiv \frac{1}{\bar{D}} \left(\frac{1}{2} - \frac{\bar{V}'}{\bar{V}} \right), & \bar{T}(\bar{z}) &\equiv \frac{\bar{V}^2 (1 + \bar{D} + \bar{D}')}{2\bar{D}}, \\ \bar{M}(\bar{z}) &\equiv (\bar{\phi} - \bar{V}^{-4} \bar{T}^2)^{\frac{1}{2}}. \end{aligned} \right\} \quad (2.14)$$

Then

$$q_0(\bar{z}) = \left(\frac{\bar{c} - \bar{T}}{\bar{V}^2} \right)^2 + \bar{M}^2 - \bar{m}^2, \quad (2.15)$$

$$q_2(\bar{z}) = -\frac{\bar{c}}{\bar{V}^2} - \bar{m}^2 + \bar{\phi}(1 - \bar{\phi}) + \bar{\phi}'. \quad (2.16)$$

Here, without loss of generality, we have set $\bar{V}(0) = 1$. Thus $V_0 = V(0)$, and Γ is the ratio of magnetic to fluid pressure at $z = 0$, a free parameter of the system; \bar{c} is the dimensionless complex wave speed along the magnetic field. The system is unstable if \bar{c} has a positive imaginary part.

It will be of use, before proceeding, to observe that (1.1) and (1.2) clearly imply

$$\int_{\bar{z}_1}^{\bar{z}_2} |f|^2 \mathcal{I}(\lambda^2 q_0 + q_2) d\bar{z} = 0. \quad (2.17)$$

3. Local stability analysis

When $|\bar{z}_2 - \bar{z}_1| \ll 1$, an approximate dispersion relation for the complex wave speed is provided by (1.6). Thus

$$\bar{c} = \bar{T} \pm i\bar{V}^2 \left(\bar{M}^2 - \bar{m}^2 - \frac{N^2\pi^2}{\lambda^2(\bar{z}_2 - \bar{z}_1)^2} \right)^{\frac{1}{2}}, \quad (3.1)$$

and the right-hand side is evaluated at $\bar{z} = \bar{z}_c$. In dimensional form

$$\omega = \frac{mV^2}{2\Omega} \left\{ \frac{g}{a^2} + \frac{V^2B'}{2a^2B} \pm i \left[-\frac{g}{a^2} \frac{d}{dz} \left[\ln \left(\frac{B}{\rho} \right) \right] - \left(\frac{V^2B'}{2a^2B} \right)^2 - m^2 \left(1 + \frac{N^2\pi^2}{k^2(z_2 - z_1)^2} \right) \right]^{\frac{1}{2}} \right\}. \quad (3.2)$$

From (3.2) we see that ω will have a non-zero imaginary part, implying instability, if

$$\left\{ \frac{d}{dz} \left[\ln \left(\frac{B}{\rho} \right) \right] \right\}_{z=z_c} < 0$$

and $|m|$ and V^2/a^2 are sufficiently small.

The terms in $V^2B'/2a^2B$ do not appear in (the Cartesian limit of) equation (4.1) of Acheson & Gibbons (1978), or in equation (3.2) of Acheson (1979) with $\eta = 0$, because it has been assumed in these papers that $V^2 \ll a^2$ throughout the fluid; these authors set $N = 1$, the most unstable value consistent with the boundary conditions. Moffatt† (1978) ignored boundary conditions and set $N = 0$; thus, according to him, the system is locally unstable at $\bar{z} = \bar{z}_0$ if

$$|\bar{m}| < \bar{M}(\bar{z}_0); \quad (3.3)$$

we shall adopt this definition of local stability here as well. Then in the limit $\lambda \rightarrow \infty$ the fluid is unstable if it is locally unstable everywhere (see the appendix).

When $|\bar{z}_1 - \bar{z}_2| \sim O(1)$, however, the estimate (3.1) of the complex eigenvalue $\bar{c} = \bar{c}_R + i\bar{c}_I$ varies significantly throughout $[\bar{z}_1, \bar{z}_2]$. Now the limit of (2.17) as $\lambda \rightarrow \infty$ is

$$c_1 \int_{\bar{z}_1}^{\bar{z}_2} \bar{V}^{-4} (\bar{c}_R - \bar{T}(\bar{z})) |f|^2 d\bar{z} = 0, \quad (3.4)$$

and if $\bar{c}_I \neq 0$ then the integrand in (3.4) must change sign. There is therefore at least one location in $[\bar{z}_1, \bar{z}_2]$ for which the *real* part of the eigenvalue is given correctly by (3.1); but this location is not necessarily the mid-point, as we shall now demonstrate.

4. Stability analysis for a deep layer: $\bar{z}_2 - \bar{z}_1 = 1$

For the numerical calculations we chose $\Gamma = 0.3$, $\bar{z}_1 = -0.5$, $\bar{z}_2 = 0.5$ and

$$\bar{V} = e^{-k\bar{z}}. \quad (4.1)$$

† Equation (3.2) with $N = 0$ is structurally similar though not quite identical to the one obtained by Moffatt, who bypassed the derivation of (2.6) by taking the limit $\lambda \rightarrow \infty$ in (2.4). In this way the time-dependent term in the second of (2.3) was filtered out by a secondary process, through which other terms in the last of (2.4) are ignored as well, and the magnetoacoustic speed remains a natural speed in Moffatt's analysis. The magnetoacoustic speed does not feature in our analysis because the time-dependent term in the last of (2.4) is absent. The two approaches can be reconciled by replacing $c^2 + h_0^2$ by c^2 (equivalent to replacing $a^2 + V^2$ by a^2) in Moffatt's equation (10.118), which then reduces to (3.2) above with $N = 0$.

\bar{z}	\bar{V}	$\rho_0/\rho_0(0)$	$B/B(0)$
-0.5	1.49	1.30	1.70
-0.4	1.38	1.25	1.54
-0.3	1.27	1.19	1.39
-0.2	1.17	1.13	1.25
-0.1	1.08	1.07	1.12
0.0	1.00	1.00	1.00
0.1	0.92	0.93	0.89
0.2	0.85	0.87	0.79
0.3	0.79	0.80	0.71
0.4	0.73	0.74	0.63
0.5	0.67	0.68	0.55

TABLE 1. Variation with height \bar{z} of density ρ_0 and magnetic field B

The corresponding equilibrium magnetic field and density are clearly given by

$$\left. \begin{aligned} B(\bar{z}) &= B(0) \exp \left[- \int_0^{\bar{z}} \frac{d\xi}{H_B} \right], \\ \rho_0(\bar{z}) &= \rho_0(0) \exp \left[- \int_0^{\bar{z}} \frac{d\xi}{H_\rho} \right], \end{aligned} \right\} \quad (4.2)$$

where $\bar{D}(\xi) = 1 + \frac{3}{2} e^{-\frac{8}{5}\xi}$ and $10\bar{D} = 13H_B = 2(13 - 8\bar{D})H_\rho$, and are tabulated in table 1. Note that the density decreases with height less rapidly than the magnetic field, a necessary condition for instability according to (3.2).

First we solved (1.1) and (1.2) for $\bar{m} = 0.5$ and various values of λ . A shooting method was used: (1.1) was rewritten as four first-order equations for the real and imaginary parts, and their derivatives, of $f = f_R + if_I$; \bar{c} was guessed; (1.1) was integrated subject to the initial conditions

$$\left. \begin{aligned} f_R(\bar{z}_1) &= f_I(\bar{z}_1) = 0, \\ f'_R(\bar{z}_1) &= \beta_R, \quad f'_I(\bar{z}_1) = \beta_I, \end{aligned} \right\} \quad (4.3)$$

using Merson's method and the NAG (Numerical Algorithms Group) routine D02ABF; then \bar{c} was guessed again until it converged to the value for which $f(\bar{z}_2) = 0$. (The resulting pair of nonlinear equations for \bar{c}_R, \bar{c}_I was solved by a modified Newton-Raphson method, using NAG routine E04FDF.) We set $\beta_I = 0$ (ensuring that the eigenfunction is real if the eigenvalue is) and $\beta_R > 0$ (it is determined ultimately by normalization).

In every case we found that the iterative scheme converged to a complex eigenvalue if its real part was well guessed and its imaginary part overestimated; otherwise it converged to a real eigenvalue. The reason for this is best appreciated by considering the surface $Z = |f(\bar{z}_2)|$ as a function of \bar{c}_R and \bar{c}_I ; the eigenvalues are the points (\bar{c}_R, \bar{c}_I) where Z dips to a local minimum of zero. Each such point is located in a valley whose axis is $\bar{c}_R = \text{constant}$ (this explains why \bar{c}_R must be well guessed) and, along the axis, the valley floor rises at first from $\bar{c}_I = 0$, dips to the minimum and then rises indefinitely (this explains why \bar{c}_I must be overestimated). Thus it is more appropriate to use $N = 0$ in (3.1) than $N = 1$. The picture is symmetric about $\bar{c}_I = 0$ since the complex eigenvalues occur in conjugate pairs.

\bar{z}	$\bar{\omega}_L(\bar{z}) = \bar{m}\bar{c}_L(\bar{z})$	$\bar{\omega} = m\bar{c}$		
		$\lambda = 10$	$\lambda = 16$	$\lambda = 25$
-0.5	0.75 + 0.58i	0.71	0.73	0.66
-0.4	0.68 + 0.48i	0.71	0.61	0.58
-0.3	0.60 + 0.40i	0.51	0.61	0.60 + 0.30i
-0.2	0.54 + 0.33i	0.51	0.53 + 0.23i	0.49
-0.1	0.47 + 0.27i	0.43 + 0.14i	0.46	0.46 + 0.16i
0.0	0.42 + 0.22i	0.43 + 0.14i	0.46	0.30 + 0.03i
0.1	0.36 + 0.18i	0.43 + 0.14i	0.34 + 0.09i	0.34 + 0.08i
0.2	0.32 + 0.15i	0.51	0.34 + 0.09i	0.34 + 0.08i
0.3	0.28 + 0.12i	0.51	0.34 + 0.09i	0.30 + 0.03i
0.4	0.24 + 0.10i	0.17	0.20	0.30 + 0.03i
0.5	0.21 + 0.08i	0.17	0.20	0.30 + 0.03i

TABLE 2. Eigenvalues to which the iterative scheme converges when the local frequencies $\bar{\omega}_L(\bar{z}) = \bar{m}\bar{c}_L(\bar{z})$ in the second column are used as starting points and $\bar{m} = 0.5$; $\bar{\omega}_L(\bar{z})$ is independent of λ since $N = 0$ in (3.1). Here, as throughout the paper, all figures have been obtained to much greater accuracy but rounded for ease of presentation.

For each value of λ we repeated the calculation of the eigenvalue $\bar{\omega} = \bar{m}\bar{c}$ for eleven different initial guesses, namely the local eigenvalues $\bar{\omega}_L(\bar{z}) = \bar{m}\bar{c}_L(\bar{z})$, where $\bar{c}_L(\bar{z})$ is given by (3.1), and $\bar{z} = \bar{z}_1 + 0.1J(\bar{z}_2 - \bar{z}_1)$, $J = 0, 1, \dots, 10$. The results for $\lambda = 10, 16$ and 25 are shown in table 2. Note how the iterative scheme converges to a complex eigenvalue when the frequency is well-guessed. The calculations were also performed for stronger field gradients than that of (4.1); the same eleven initial guesses were not sufficient to locate the complex eigenvalues, because $\bar{\omega}_L(\bar{z})$ varied too rapidly (and intermediate locations had to be used). Thus the steeper the field gradient the more accurately $\bar{\omega}_R$ must be guessed.

Note also, from table 2, that the value of \bar{z} for which $\bar{\omega}_L(\bar{z})$ selects the eigenvalue with maximum growth rate migrates towards the lower boundary $\bar{z}_1 = -0.5$ as $\lambda \rightarrow \infty$. For $\lambda = 16, 25$ it is $\bar{z} = -0.2, -0.3$ and only for $\lambda \lesssim 10$ is it the mid-point $\bar{z} = 0$. Since $\bar{\omega}_R$ must be well-guessed, and $\bar{\omega}_R(\bar{z})$ increases if \bar{z} decreases, this simply means that the frequency corresponding to maximum growth rate increases with λ ; but the reason for this, in turn, can be appreciated upon inspection of figure 1. Here the eigenfunction f corresponding to maximum growth rate is plotted for $\lambda = 10, 25$. It is clear that the peak which gives the maximum contribution to $|f|^2$ is migrating towards $\bar{z}_1 = -0.5$ as $\lambda \rightarrow \infty$ and oscillations increase; on the other hand, it can easily be shown that $\bar{T}(\bar{z})$, defined by (2.14), decreases monotonically with \bar{z} for fields of the form (4.1). Thus $\bar{c}_R - \bar{T}(\bar{z})$ can (and must) vanish only once, changing sign from negative to positive; and this point must migrate towards \bar{z}_1 as λ increases to balance out the positive and negative contributions to the integral (3.4).

By fixing λ and plotting growth rate $\bar{\omega}_I$ versus wavenumber \bar{m} we obtained the critical wavenumber, $\bar{m}_c(\lambda)$, which is the maximum for instability; figure 2 is typical. Then by varying λ we obtained \bar{m}_c as a function of \bar{k} . The results are presented in figure 3, where the region above the solid curve corresponds to instability; no complex eigenvalues were found for $\lambda < 4.7$.

The vertical broken lines are given by $\bar{m} = 0.61, 0.72$, the minimum and maximum values of $\bar{M}(\bar{z})$ in $[-0.5, 0.5]$. To the left of $\bar{m} = 0.61$, the system is locally unstable

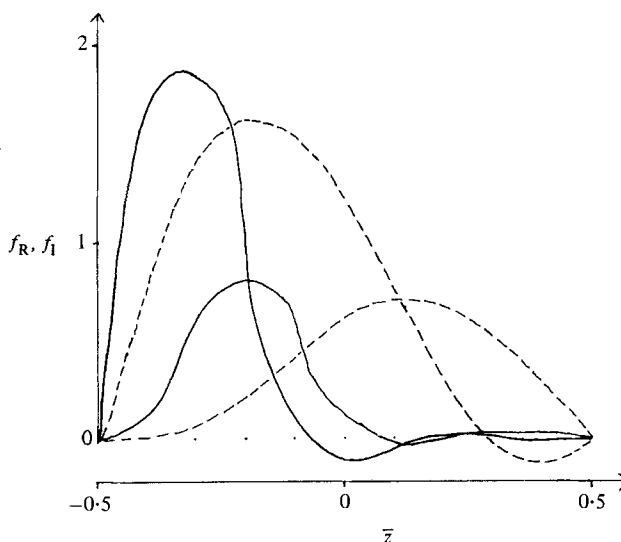


FIGURE 1. Eigenfunctions $f(\bar{z})$ for $\lambda = 10$, $\bar{\omega} = 0.43 + 0.14i$ (broken curve) and $\lambda = 25$, $\bar{\omega} = 0.6 + 0.3i$ (solid curve). In each case $f_R(\bar{z})$ has the more prominent peak while $f_I(\bar{z})$ has zero gradient at $\bar{z} = -0.5$.

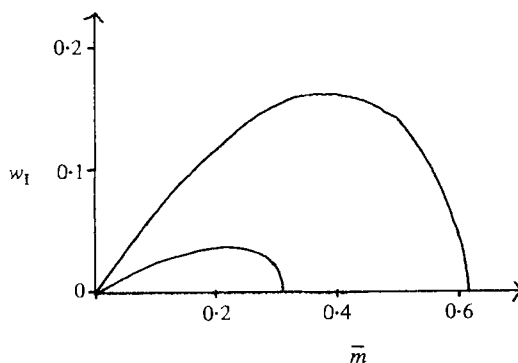


FIGURE 2. Growth rate $\bar{\omega}_I$ as a function of \bar{m} . Here $\lambda = 10$, there are two branches and $\bar{m}_c = 0.62$. The number of branches and maximum growth rate increase with λ ; an absolute maximum cannot be calculated because dissipative processes have been ignored.

everywhere according to (3.3); to the right of $\bar{m} = 0.72$ it is locally stable everywhere. Thus there is a region, shaded in the diagram, for which the fluid is unstable even though it is locally stable in part of the interval $[-0.5, 0.5]$.

Finally, the sloping broken line is the ray $\lambda = \bar{k}/\bar{m} = 9.5$. Thus, for $\lambda > 9.5$, the fluid is unstable if it is locally unstable everywhere. For $\lambda \rightarrow \infty$, the same result is proved analytically in the appendix.

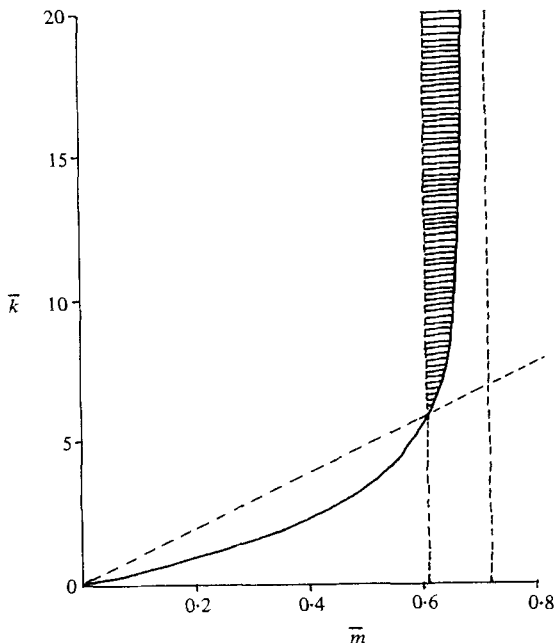


FIGURE 3. Stability diagram in the (\bar{m}, \bar{k}) -plane. The picture is symmetric about $\bar{m} = 0$ (since complex eigenvalues occur in conjugate pairs) and about $\bar{k} = 0$ (since the sign of \bar{k} does not matter anyway). For a description see the last two paragraphs of § 4.

5. Conclusions

The stability has been considered of a deep,† rotating layer of inviscid, isothermal, compressible fluid which is permeated by a non-uniform horizontal magnetic field. This layer (described in § 2) is unstable (see § 4) to perturbations whose wavelength $2\pi/m$ along the field is sufficiently long compared with the normal wavelength $2\pi/k$, when the magnetic field strength falls off with height more rapidly than the fluid density. In this respect the stability of the fluid is predicted adequately by the local (shallow-layer) analysis of Moffatt (1978, § 10.7) and Acheson & Gibbons (1978).

When the frequencies and growth rates of the unstable modes for a deep layer are sought, however, the local stability analysis must be applied with caution. The local dispersion relation (1.6) should be evaluated at a point z_0 which is not necessarily the mid-point but migrates towards the lower boundary (i.e. towards regions of higher local Alfvén speed $V(z)$) as k/m increases towards infinity; z_0 is also the point around which the amplitude of the eigenfunction is concentrated. Provided these details are observed, the local eigenvalues ω_L provide good initial guesses for a numerical scheme to determine the complex eigenvalues of (1.1) and (1.2); the scheme requires that the real part of the initial guess ω_L match the true frequency ω_R rather well and that the imaginary part of the initial guess be an overestimate of the true growth rate ω_I .

The author is grateful to several referees of previous versions of this paper for their comments and to the Deutscher Akademischer Austauschdienst for financial support.

† The results would not be altered qualitatively if the layer were deeper than one isothermal scale height, but the assumption of constant gravity would be called into question.

Appendix. Local instability everywhere implies instability

We show that the system described in §2 and governed by (1.1)–(1.2) is unstable as $\lambda \rightarrow \infty$ if it is locally unstable everywhere, and \bar{T} , defined in (2.14), is a monotonically decreasing function of \bar{z} . The latter condition was sufficiently general to cover all fields considered in the numerical work.

Assume $\bar{c}_I \neq 0$ and resolve (2.15) into its real and imaginary parts:

$$\left. \begin{aligned} q_{0R}(\bar{z}) &= \bar{V}^{-4} \{ (\bar{c}_R - \bar{T}(\bar{z}))^2 - \bar{c}_I^2 \} + (M(\bar{z}))^2 - \bar{m}^2, \\ q_{0I}(\bar{z}) &= 2\bar{c}_I \bar{V}^{-4} (\bar{c}_R - \bar{T}(\bar{z})). \end{aligned} \right\} \quad (\text{A } 1)$$

The condition on \bar{T} ensures that (see (3.4)) there is a point at which q_{0I} changes sign from negative to positive. Let ξ be this point, and consider the function

$$\begin{aligned} F(\xi) &\equiv \mathcal{I} \int_{\bar{z}_1}^{\bar{z}_2} q_0^{\frac{1}{2}} d\bar{z} \\ &= - \int_{\bar{z}_1}^{\xi} I(\bar{z}, \xi) d\bar{z} + \int_{\xi}^{\bar{z}_2} I(\bar{z}, \xi) d\bar{z}, \end{aligned} \quad (\text{A } 2)$$

where

$$I(\bar{z}, \xi) \equiv (-q_{0R} + |q_{0R}^2 + q_{0I}^2|^{\frac{1}{2}})^{\frac{1}{2}} \quad (\text{A } 3)$$

is a function of ξ as well as of \bar{z} , since $\bar{c}_R = \bar{T}(\xi)$ in (A 1). Since $F(\bar{z}_1) = -F(\bar{z}_2)$, Rolle's theorem ensures that the imaginary part of (1.5) is satisfied provided that F is continuous; the real part of (1.5) can always be satisfied for any $\bar{c}_I > 0$ since N/λ is arbitrary. But F is differentiable, and therefore continuous, as long as $q_{0R} > 0$ for all $\bar{z}_1 \leq \bar{z} \leq \bar{z}_2$; and this will be true for some $c_I > 0$, however small, if (3.3) is satisfied everywhere.

REFERENCES

- ACHESON, D. J. 1978 *Phil. Trans. R. Soc. Lond. A* **289**, 459–495.
 ACHESON, D. J. 1979 *Solar Phys.* **62**, 23–50.
 ACHESON, D. J. & GIBBONS, M. P. 1978 *J. Fluid Mech.* **85**, 743–757.
 MOFFATT, H. K. 1978 *Magnetic Field Generation in Electrically Conducting Fluids*. Cambridge University Press.
 NAYFEH, A. H. 1973 *Perturbation Methods*. John Wiley.